A Compact Microstrip-fed Planar Dual-Dipole Antenna for Broadband Applications

Boon-Kok Tan, Stafford Withington, *Member, IEEE,* and Ghassan Yassin, *Member, IEEE,*

***Abstract*—We present a broadband end-fire planar circuit antenna that is suitable for applications in microwave, millimetre (mm) and sub-millimetre (sub-mm) wavelengths. We have cascaded two dipoles of different lengths in series to broaden the bandwidth. Two printed directors and a truncated ground plane are used to achieve high front-to-back (F/B) gain ratio. The parallel stripline feeding the antenna's drivers is connected directly to microstrip without an intermediate stage. This simple antenna design is easily integrated into microstrip circuits. In this paper, we focus on the design of a Ku-band antenna with 7 GHz bandwidth and F/B gain ratio of ∼18 dB. Design and analysis of the antenna were performed using rigorous electromagnetic simulations, and we experimentally validated the performance of the antenna by measuring the beam patterns and return loss of an antenna fabricated on a Roger RO 4350 printed circuit board. Finally, we present two unique example applications of the antenna in the sub-mm detectors area.**

***Index Terms*—Microstrip antennas, Planar antennas, Ultra wideband antennas, Yagi-Uda arrays, Phased arrays.**

I. Introduction

MICROSTRIP-fed printed circuit antennas with end-fire beam characteristics are useful for a wide range of applications. Many types of planar end-fire antenna have been developed in the past few years [1], [2], [3], but they are often fed with a slotline or a coplanar waveguide (CPW) which are not the most common form of transmission lines used in microwave circuits, which is the microstrip. A desirable microstrip-fed planar antenna, on the other hand, often requires a complicated balun as a transition stage [4], [5], which could introduce ohmic and reflection losses.

In this paper, we describe a planar microstrip antenna that has a high quality radiation pattern across a large operating bandwidth. It is compact and easy to fabricate. We use a dual-dipole configuration to broaden the operational bandwidth. These dipoles are fed directly by microstrip, hence are readily integrated into the microwave circuits. We will present in details the design of an antenna that operates in the Ku-band. All the simulations were performed using the 3-D electromagnetic package, High Frequency Structure Simulator (HFSS), to accurately model the antenna elements and optimisations.

II. Antenna design

A basic type of a free-space planar antenna is a uniplanar dipole fed with a coplanar stripline (CPS). This simple antenna structure however, requires a complicated CPS-to-microstrip balun to transform the RF signal into the microstrip circuit [5], and a single dipole antenna suffers from narrow bandwidth operation. To broaden the bandwidth, we cascade two dipoles of different lengths in series to create two resonances centred at two slightly different frequencies [6], forming a truncated log-periodic-like antenna as shown in Fig. 1. The biplanar drivers are fed with a parallel stripline, where the top stripline is connected to one half of the dipoles and the bottom stripline is connected to the other half, forming two back-to-back 'F-shapes' structures separated by a thin dielectric layer. To improve the F/B gain ratios and to obtain the end-fire far field beam patterns, we employ two planar directors located before the dual-dipole driver and a truncated ground plane as a reflecting element by extending the bottom stripline all the way to the edges. This forms a transition from the parallel stripline to a microstrip line.

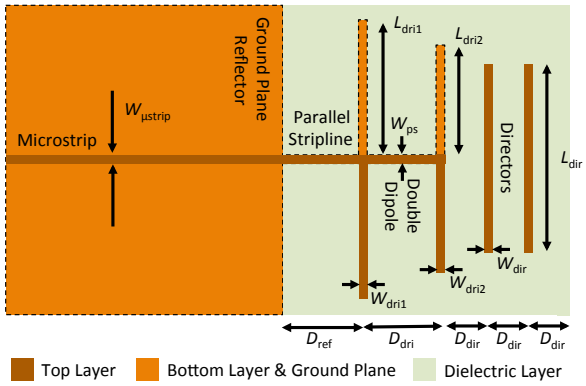

Fig. 1. Layout of the planar circuit antenna utilising a pair of dipole drivers, and the critical dimensions dictating the performance of the antenna.

A preliminary design is obtained by realising that the operating frequency and the bandwidth of the antenna are mainly determined by the two quarter-wavelength dipoles ($L_{\rm dri1}$ and $L_{\rm dri2}$, see Fig. 1). The shorter and the longer dipoles determine the higher and the lower frequency resonances respectively. The antenna gain and the return loss are determined by the distance between the two dipoles ($D_{\rm dri}$) and by the length of the parallel stripline that connect the back dipoles and the ground plane ($D_{\rm ref}$). The width of the parallel stripline ($W_{\rm ps}$) controls the output impedance and should therefore be adjusted to match the output impedance of the dual-dipole. All these dimensions, including the length of the directors ($L_{\rm dir}$) are then optimised using HFSS for the required bandwidth and radiation patterns.

B-K. Tan and G. Yassin are with the Department of Physics (Astrophysics), University of Oxford, Denys Wilkinson Building, Keble Road, OX1 3RH, Oxford, UK. E-mail: tanbk@astro.ox.ac.uk

S. Withington is with the Cavendish Laboratory, University of Cambridge, J. J. Thomson Avenue, Cambridge CB3 0HE, UK.

Manuscript received XXXX XX, 2015; revised XXXX XX, 2015.

III. Testing of a Ku-Band Dual-Dipole Antenna

Based on this method, we have designed and fabricated an antenna that can efficiently transmit/receive RF signals in the Ku-band (11–18 GHz). The antenna was printed on both sides of a 254 μm thick Roger RO 4350 substrate (dielectric constant = 3.66), and the microstrip was connected to a standard SMA connector as shown in Fig. 2. The final geometry of the optimised antenna is given in Table I. To match the antenna to the impedance of the SMA connector (50 Ω), two additional microstrip sections were added (0.4 mm and 0.5 mm wide, respectively) after the output port of the antenna to form a quarter-wavelength matching transformer.

Fig. 3 shows the HFSS simulated far field radiation pattern of the antenna at the designated central frequency 15 GHz. Both E- and H-plane radiation patterns show end-fire beam characteristics, with an approximately 18 dB F/B gain ratio. The –3 dB (full-width half-maximum, FWHM) beam width of the E-plane pattern is approximately 70° at 15 GHz, while the H-plane FWHM beam is slightly larger at approximately 110° due to the lack of conducting elements perpendicular to the antenna's plane.

The return loss of the antenna was measured using a vector network analyser (VNA) in conjunction with an Anritsu universal test fixture. The antenna (without the SMA connector) was aligned and held to the test fixture's K-connector pin using a spring-loaded jaw, and the setup was screened with high loss microwave absorbers to eliminate reflection interference. In Fig. 4, we show that the measured return loss of the antenna agrees exceedingly well with the HFSS simulated result. All the measured resonance dips follow almost exactly the design frequency positions, except that the measured upper frequencies and resonance (around 17.5 GHz) are slightly lower than predicted. Nevertheless, the return loss remains below –9 dB in a frequency range of 11–18 GHz,

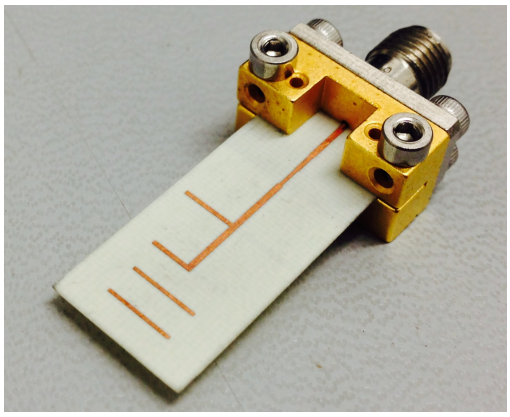

Fig. 2. A Ku-band dual-dipole antenna fabricated on a 254 μm thick Roger RO 4350 printed circuit board.

TABLE I
Dimensions of the optimised Ku-band dual-dipole antenna. All dimensions are in mm.

L_{dri1}	5.00	W_{dri1}	0.35	D_{ref}	5.50	W_{ps}	0.50
L_{dri2}	3.65	W_{dri2}	0.40	D_{dri}	4.95	W_{ustrip}	0.30
L_{dir}	5.75	W_{dir}	0.30	D_{dir}	2.50	(Z_{out}	40 Ω)

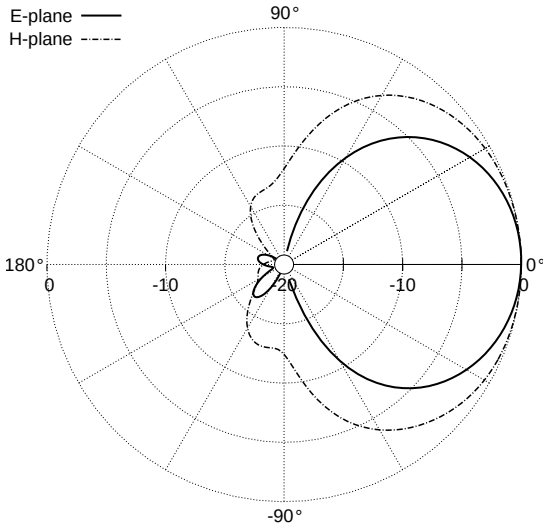

Fig. 3. Far field radiation pattern of the planar dual-dipole antenna at its central frequency (15 GHz), simulated with HFSS including the 50 Ω microstrip transition.

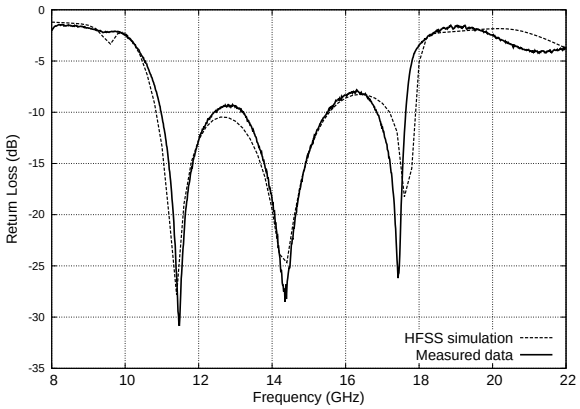

Fig. 4. The measured return loss performance of the Ku-band dual-dipole antenna in comparison to the HFSS predicted performance.

corresponding to a bandwidth of approximately 1.64:1 (48%).

The far field radiation patterns of the antenna were measured in a test range equipped with a rotary table in an anechoic chamber. The antenna under test was used as a transmitter with an RF signal fed from the first test port of the VNA. A 15 GHz horn antenna connected to the second test port of the VNA was aligned and placed approximately 2 meters ($\sim 100\ \lambda$, much larger than the Rayleigh distance) away from the antenna under test to measure the far field radiated RF power. The radiation patterns were then obtained by logging the signal received from the horn antenna while rotating the transmitter under computer control.

Fig. 5 shows the measured far field beam patterns of the antenna at the central frequency, and at the edges of the frequency band. The measured E- and H-plane beam patterns match very well the HFSS predictions across the whole frequency band. In fact, the measured and the calculated beam patterns are indistinguishable down to –10 dB level. The good agreement holds up to the high frequency end (e.g., 17 GHz). Above this frequency, the measured main beams

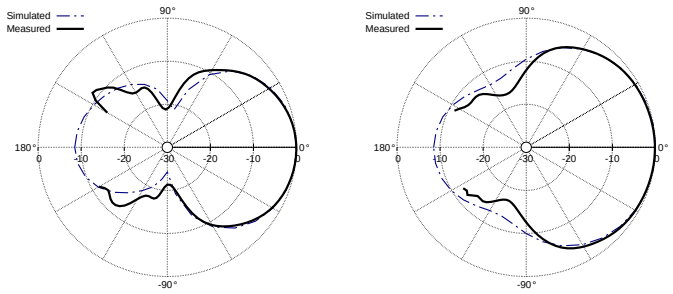

(a) 11 GHz E-plane (b) 11 GHz H-plane

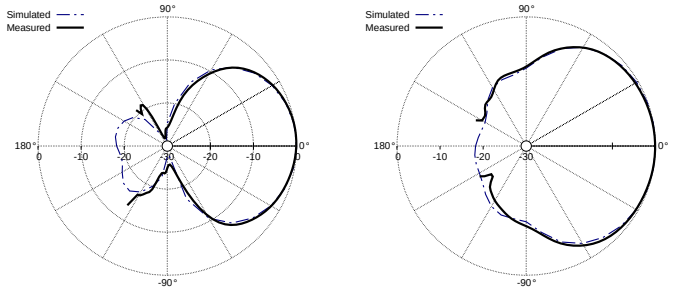

(c) 15 GHz E-plane (d) 15 GHz H-plane

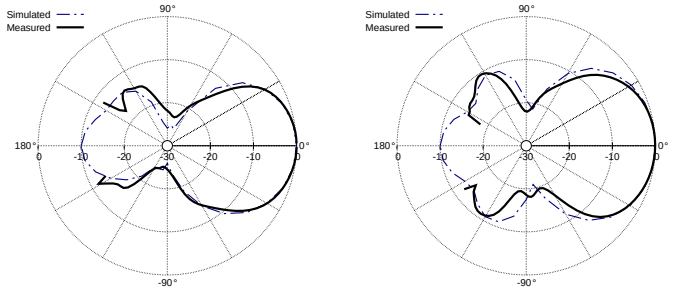

(e) 17 GHz E-plane (f) 17 GHz H-plane

Fig. 5. E- and H-plane far-field radiation patterns of the antenna measured (solid line) in a 5 GHz anechoic chamber. Shown along with the measured plots are the HFSS calculated beam patterns (dashed line).

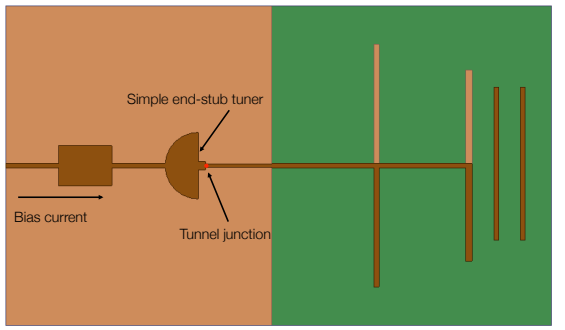

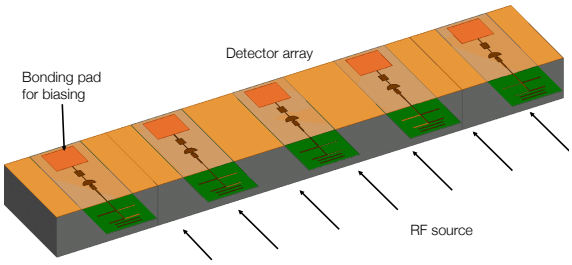

(a)

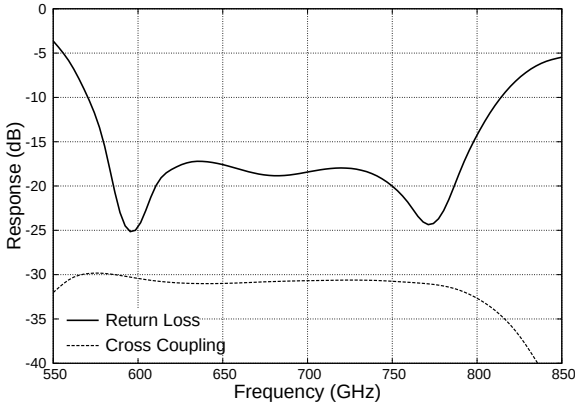

(b)

Fig. 6. (a) An array of dual-dipole antennas feeding the superconducting tunnel junctions for simultaneous DC current-voltage curves measurement. Each antenna is connected directly to a tunnel junction via a microstrip line, and a simple end-stub tuning network is used to cancel out the junction capacitance at a specific frequency. (b) The return loss bandwidth of the 700 GHz planar double-dipole antenna, and the cross-coupling of the same antenna placed adjacent to another planar dual-dipole antenna at about one wavelength (λ_0) separation distance.

become slightly narrower than the computed one.

IV. Applications at Sub-mm Wavelengths

Our motivation in developing the above-described dual-dipole antenna is to use it as a feed for the superconducting tunnel junction detectors usually developed for sub-mm astronomical receivers. These sub-mm detector chips are normally mounted in the E-plane of a rectangular waveguide of tiny dimensions ($\sim$ 100 μm) and the RF power from the waveguide is coupled to the device via a waveguide-to-microstrip transition (see e.g., [7], [8]). Considerable effort is therefore required to fabricate the detector block and to mount each detector chip accurately in the waveguide. This is in particular time-consuming during the initial testing of a new generation of detector devices since intensive repeated testings are required to characterise and understand their properties. It would therefore be much more convenient to fabricate an array of detectors, each fed by a free-space dual-dipole antenna as shown in Fig. 6 (a), and test these detector devices simultaneously by illuminating the array with a sub-mm source at a required frequency [9]. The detector array can be fabricated using deposition and photolithography processing on a single wafer, allowing an easy and fast characterisation of the new detector design.

TABLE II
Dimensions of the optimised dual-dipole antenna at 700 GHz. All dimensions are in μm.

L_{dri1}	92.5	W_{dri1}	4.0	D_{ref}	80.5	W_{ps}	3.0
L_{dri2}	73.0	W_{dri2}	5.0	D_{dri}	70.0	$W_{\mu strip}$	2.2
L_{dir}	115.0	W_{dir}	3.5	D_{dir}	20.0	(Z_{out}	40 Ω)

For this purpose, we have scaled and optimised the dual-dipole antenna to operate at the 700 GHz frequencies range. The antenna was formed using a 400 nm thick niobium nitride

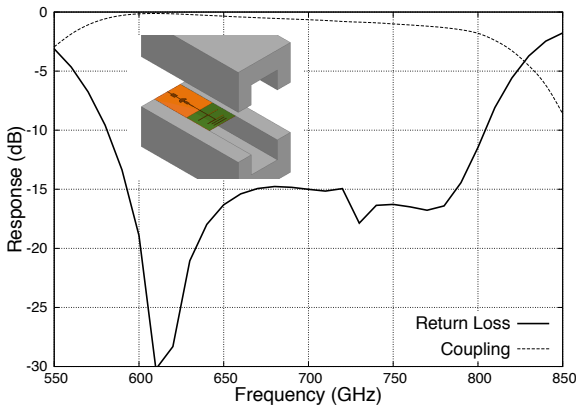

Fig. 7. The coupling and return loss performance of the dual-dipole antenna as a waveguide-to-microstrip transition at sub-mm frequencies. The waveguide height was over-sized slightly to accommodate the length of the dipoles.

superconducting film as the top metallisation layer and a niobium thin film of the same thickness as the bottom layer, with a 460 nm silicon dioxide as the insulating layer. The entire antenna structure was fabricated on a 1 μm thick silicon nitride membrane on top of a 200 μm silicon substrate, which is etched away at the end of the processing. The 1 μm chip is then mounted at the E-plane of a rectangular waveguide. The optimised geometry for the sub-mm antenna is summarised in Table II. As shown in Fig. 6 (b), the sub-mm antenna have the same large operational bandwidth with a return loss better than –15 dB from 580–800 GHz. The cross-coupling between two antennas placed at about one wavelength (400 μm) away from each other along the antenna plane is shown to be less than 0.1% across the band. The cross-coupling increases to about –20 dB if the separation between the two antennas is halved to $\lambda_0/2$. The radiation pattern of the individual antenna in this two-element array also remain largely unchanged from the single-element antenna.

Another attractive application of the antenna in the sub-mm detectors area is to use it as a transition from waveguide to planar circuit. This is an important component in mm and sub-mm astronomical receivers as the RF signal is collected by an electromagnetic horn and coupled to a detector chip from the waveguide. The advantages of the dual-dipole antenna in this application over the commonly used radial probe [10], [11] are that it has an input impedance comparable to the unloaded waveguide. It can easily be grounded to the waveguide and it does not require the fabrication of a precisely machined backshort. Fig. 7 shows the simulated power coupling and return loss performance of a dual-dipole antenna positioned at the E-plane of a rectangular waveguide, which shows that it can be used as a high performance waveguide-to-planar-circuit transition at mm and sub-mm wavelengths.

V. Conclusion

We have presented the design and the experimentally measured performance of a planar end-fire antenna that is compact and compatible with microwave circuit technology. We cascaded two dipoles to achieve broadband operation, and utilised a truncated ground plane and two printed directors to achieve high F/B gain ratio and end-fire far field radiation characteristic. The antenna has a very simple geometry, and is fed directly by microstrip line. We fabricated a Ku-band antenna based on this design and measured the far field beam patterns and return loss performance. The measured results agreed very well with the simulated performance. Although the integrity of the design was demonstrated at microwave frequencies, our simulations show that it has attractive applications at sub-mm wavelengths, both as a free space antenna and as a waveguide-to-microstrip transition.

References

[1] G. Zheng, A. Kishk, A. Glisson, and A. Yakovlev, "Simplified feed for modified printed Yagi antenna," *Electronics Letters*, vol. 40, no. 8, pp. 464–466, 2004.

[2] G. DeJean and M. Tentzeris, "A New High-Gain Microstrip Yagi Array Antenna With a High Front-to-Back (F/B) Ratio for WLAN and Millimeter-Wave Applications," *Antennas and Propagation, IEEE Transactions on*, vol. 55, no. 2, pp. 298–304, 2007.

[3] Y. Liu, L.-M. Si, M. Wei, and et al., "Some Recent Developments of Microstrip Antenna," *International Journal of Antennas and Propagation*, vol. 2012, pp. 1–10, 2012, 428284.

[4] N. Kaneda, Y. Qian, and T. Itoh, "A broad-band microstrip-to-waveguide transition using quasi-Yagi antenna," *Microwave Theory and Techniques, IEEE Transactions on*, vol. 47, no. 12, pp. 2562–2567, 1999.

[5] N. Kaneda, W. Deal, Y. Qian, R. Waterhouse, and T. Itoh, "A broadband planar quasi-Yagi antenna," *Antennas and Propagation, IEEE Transactions on*, vol. 50, no. 8, pp. 1158–1160, 2002.

[6] A. A. Eldek, "Design of double dipole antenna with enhanced usable bandwidth for sideband phased array applications," *Progress In Electromagnetics Research*, vol. 59, pp. 1–15, 2006.

[7] J. Zmuidzinas and P. L. Richards, "Superconducting detectors and mixers for millimeter and submillimeter astrophysics," *Proceedings of the IEEE*, vol. 92, no. 10, pp. 1597–1616, 2004.

[8] B.-K. Tan, G. Yassin, P. Grimes, and K. Jacobs, "650 GHz SIS mixer fabricated on silicon-on-insulator substrate," *Electronics Letters*, vol. 49, no. 20, pp. 1273–1275, September 2013.

[9] B.-K. Tan, G. Yassin, S. Withington, and D. Goldie, "Broadband Planar Yagi Antenna for Millimetre & Sub-millimetre Detectors," in *Millimeter Waves and THz Technology Workshop (UCMMT), 2013 6th UK, Europe, China*, Sept. 2013, pp. 1–2.

[10] J. Kooi, G. Chattopadhyay, S. Withington, F. Rice, J. Zmuidzinas, C. Walker, and G. Yassin, "A full-height waveguide to thin-film microstrip transition with exceptional rf bandwidth and coupling efficiency," *International Journal of Infrared and Millimeter Waves*, vol. 24, no. 3, pp. 261–284, 2003.

[11] S. Withington, J. Leech, G. Yassin, K. Isaak, B. Jackson, J. Gao, and T. Klapwijk, "A 350ghz radial-probe sis mixer for astronomical imaging arrays," *International Journal of Infrared and Millimeter Waves*, vol. 22, no. 9, pp. 1305–1312, 2001.